Journal of Diabetes and Its Complications 33 (2019) 374–382

Contents lists available at ScienceDirect

Journal of Diabetes and Its Complications

journal homepage: WWW.JDCJOURNAL.COM

Hyperglycemia inhibition of endothelial miR-140-3p mediates angiogenic dysfunction in diabetes mellitus

Dongni Wang [a], Haiyan Wang [a], Cun Liu [a], Xiaofeng Mu [b], Shaoyun Cheng [a,*]

[a] Department of Clinical Laboratory, The 3rd People's Hospital of Qingdao, Qingdao 266041, Shandong Province, China
[b] Department of Clinical Laboratory, Qingdao Central Hospital, Qingdao 266042, Shandong Province, China

ARTICLE INFO

Article history:
Received 5 September 2018
Received in revised form 13 January 2019
Accepted 3 February 2019
Available online 10 February 2019

Keywords:
Diabetes mellitus (DM)
miRNA
Hyperglycemia
FOXK2
Angiogenesis

ABSTRACT

Objective: MicroRNAs (miRNAs) have emerged as promising regulators of diabetes mellitus (DM)-induced angiogenic dysfunction in endothelial cells (ECs), but information vis-à-vis the functional roles of distinct miRNAs remain surprisingly scarce. The current study was designed to elucidate the expression and function of miR-140-3p in diabetic ECs.
Methods: miR-140-3p expression was evaluated in DM mouse model and in human ECs using RT-qPCR, Northern blot and RNA fluorescent *in situ* hybridization. Effects of miR-140-3p manipulation on ECs function were evaluated using cell proliferation, migration and *in vitro* tube formation assay. Regulation of FOXK2 transcription by miR-140-3p was determined by luciferase reporter assay and site-directed mutagenesis.
Results: miR-140-3p expression was significantly down-regulated in high glucose-challenged ECs. Under normal conditions, miR-140-3p knockdown impaired endothelial proliferation and migration, and endothelial tube formation. Mechanistically, miR-140-3p exhibited its proangiogenic effects through directly inhibiting the expression of the forkhead transcription factor FOXK2. From a therapeutic standpoint, shRNA-mediated stable inhibition of FOXK2 effectively corrected miR-140-3p deficiency–induced impairment of ECs proliferation and *in vitro* angiogenesis.
Conclusion: Endothelial miR-140-3p positive regulates ECs function by directly targeting FOXK2 signaling. Deregulation of miR-140-3p/FOXK2 cascade by hyperglycemia thus serves as an important contributor to angiogenic dysfunction in DM.

1. Introduction

In conjunction with urbanization and lifestyle changes, diabetes mellitus (DM) is currently a leading cause of metabolic disorders.[1] Globally, the victims of DM is estimated to be around 642 million by 2040.[2] Regardless of clinicopathological categorization, both type 1 and type 2 diabetes result in marked plasma hyperglycemia.[3,4] Within the vasculature, the endothelial cells (ECs) remain the main targets of glucose-mediated challenges. Intracellular hyperglycemia induces endothelial dysfunction and microvascular rarefaction. Given that smallest blood vessels play essential roles in nourishing multiple organs, microangiopathy serves as a major risk factor for diabetic complications causing more than half of morbidity and mortality in diabetic patients.[5] Despite such pervasiveness, the underlying mechanisms for ECs dysfunction in DM remain poorly understood.

MicroRNAs (miRNAs), a group of small, noncoding RNAs that mediate degradation of targeted mRNA and/or translational arrest by binding to specific sequences (such as 3′ untranslated region, 3′-UTR). The expression of >30% of human genes is regulated by miRNAs at the post-transcriptional level.[6] Of particular interest, miRNAs are gradually regarded as important contributing factors for angiogenic dysfunction in DM.[7–9] For instance, miR-27b rescues bone marrow-derived angiogenic cell function in T2DM.[10] Down-regulation of miR-126 and miR-132 are functionally implicated in diabetic cardiac microangiopathy and these two miRNAs are thus considered to be important proangiogenic factors.[11] We have previously reported that T2DM inhibition of endothelial miR-342-3p facilitates angiogenic dysfunction *via* repression of FGF11 signaling.[12] Hitherto, the expression, functions, and targets of miRNAs in ECs remain largely unexplored.

In the present study, miR-140-3p was chosen for further investigation based on three criteria: i) miR-140-3p has been shown by comparative miRNA array analysis to be a signature miRNA in hyperglycemic conditions.[13] ii) miR-140-5p, another isoform of miR-140, has been reported to regulate angiogenesis in both normal[14] and transformed cells.[15] iii) translational relevance of circulating miR-140-3p as a potential biomarker for monitoring metabolic processes has been proposed

* Corresponding author at: Department of Clinical Laboratory, The 3rd People's Hospital of Qingdao, No.29, Yongping Road, Licang District, Qingdao 266041, Shandong Province, China.
E-mail address: chengshaoyun@126.com (S. Cheng).

https://doi.org/10.1016/j.jdiacomp.2019.02.001
1056-8727/

by multiple publications.[16,17] In an exploration of the mechanisms underlying miR-140-3p action, we demonstrate that deregulation of miR-140-3p/FOXK2 cascade by hyperglycemia exacerbates the primary ECs dysfunction and attenuates *in vitro* angiogenesis, thus indicating a novel proangiogenic facet of miR-140-3p.

2. Materials and methods

2.1. Patient samples and animal models

The human study, strictly conformed to the ethical standards of *Helsinki Declaration*, was approved by the Clinical Investigation Committee of our hospital (QDRMYY-20160618-098). All participants gave informed consent before inclusion. Peripheral blood samples, along with human $CD34^+$ cells purified from these blood samples, were obtained from healthy volunteers ($n = 15$) and T2DM patients ($n = 18$), as described in detail in our previous work.[12] Moreover, patients with glaucoma (diagnosed as glaucomatous optic neuropathy by fundoscopic examination with elevated intraocular pressure > 21 mmHg,[18] $n = 12$), with cataract ($n = 8$), or with diabetic retinopathy (DR, $n = 16$) were recruited from Department of Ophthalmology in 3rd People's Hospital of Qingdao during September 2016 and April 2017. ~100 μl of aqueous humor (AH) samples, collected from anterior chamber paracentesis from these ophthalmic patients, were stored immediately at −80 °C until further use.

The animal work, in accordance with the *Guide for the Care and Use of Laboratory Animals published by the National Institutes of Health* (NIH publication No. 85–23, revised 1996), was approved by the Animal Care and Use Committee of our hospital (QDRMYY-20160618-096). Adult C57/BL6 male mice at the ages of 2 months were obtained from the Animal Research Center of our hospital. Mice had free access to clean water and were fed *ad libitum*, and maintained under a constant 12 h light:12 h darkness cycle (lights on at 0800 h) and controlled conditions of humidity (between 70 and 80%) and temperature (22 ± 1 °C). Mice were sacrificed by CO_2 inhalation followed by cervical dislocation and all efforts were made to minimize suffering. To induce T2DM, mice ($n = 10$) were fed on a high fat diet (HFD) (Jiangsu Medicience Biomedicine, Yangzhou, China). Three weeks later, mice were injected intraperitoneally with a single dose of of STZ (80 mg/kg in 0.1 M citrate buffer, pH 4.5, Sigma-Aldrich, Beijing, China). Mice fed on a normal diet served as the control ($n = 10$). Three weeks after the STZ injection, mice with distinct hyperglycemia concomitant with insulin resistance (beyond 1–2 S.D. values from the normal controls) were considered as T2DM.[19]

2.2. Cell treatment

Human retinal vascular endothelial cells (HRVECs), human umbilical vein endothelial cells (HUVECs), human coronary artery endothelial cells (HCAECs) and human coronary artery endothelial cells (EA.hy.926) were obtained from ATCC (Manassas, VA, USA). These purchased endothelial cells (passage 3-6) were cultured at 37 °C with 5% CO_2 in EGM2-MV media supplemented with different doses of FBS (5% of FBS for HRVECs, 2% FBS for HUVECs and HCAECs, and 10% of FBS for EA.hy.926) (Gibco, Shanghai, China), according to the procedures suggested by ATCC. Primary ECs were isolated and purified from heart tissues using a sequential affinity selection method, as described in our previous work.[12] The primary ECs lineage was further confirmed by analyzing primary ECs (at subculture <2) for cell surface expression of PECAM-1 and ICAM-2, the two endothelial-specific markers that were used for the positive selection of these cells.[20] To study the effects of hyperglycemia on miR-140-3p expression, HUVECs were incubated with the culture media containing 5 mmol/L glucose, 30 mmol/L glucose, or 30 mmol/L mannitol (osmolar control group, Sigma-Aldrich, Shanghai, China) for 4 h,[21] followed by RT-qPCR analysis. To manipulate the miR-140-3p expression, primary ECs were transfected with miR-140-3p mimics or inhibitors, along with their corresponding negative controls (RiboBio, Guangzhou, China), using HiPerFect Transfection Reagent (Qiagen, Shanghai, China). HUVECs were stably deprived of endogenous FOXK2 expression by transfection with FOXK2 shRNA (Sigma-Aldrich), followed by selection with 0.5 μg/ml G418 (Invitrogen, Shanghai, China).

2.3. Measurement of cell proliferation and migration

Primary ECs with different transfections were fixed using 10% trichloroacetic acid at 4 °C for 1 h, followed by sequential incubation with Sulforhodamine-B (Sigma-Aldrich) for 0.5 h and unbuffered Tris Base (10 mM, pH 10.5) for 5 min. Final spectrophotometry was performed at 492 nm.[12]

To measure cell migration, primary ECs with different transfections were cultured to confluence, followed by streaking at 1-mm width using a rubber scraper. 36 h later, the migrated cells beyond the streak edge were calculated in 5 random fields.[12]

2.4. Tube formation assay

Primary ECs or HUVECs with different transfections were seeded at density of 1×10^5 cells/well on a 24-well plate coated with growth factor-reduced Matrigel (300 μl/well, BD Biosciences, Shanghai, China). After incubation at 37 °C for 24 h, tube construction was viewed and tube length was quantified using Image J[22] (www.imagej.net).[23]

2.5. RT-qPCR

Total RNA was isolated using a miRNeasy Mini Kit (Qiagen, Shanghai, China) and was reverse transcribed using miScript II RT Kit or Omniscript RT Kit (Qiagen). To determine the expression levels of miR-140-3p and *FOXK2* mRNA, cDNA was subjected to PCR using a SYBR PrimeScript miRNA or an mRNA Real-Time PCR kit (Takara, Dalian, China), with *18S*, mouse snoRNA202 and human U6 snRNA serving as internal controls. Subsequent relative quantification was performed using the comparative $^{\triangle\triangle}$Ct method.[24] Primers used were: *FOXK2* (NM_004514.3), 5′-CGAGTGATGCCATCTGACCT-3′ and 5′-AGCCATCG TAATCGCCTGAA-3′; *Foxk2* (NM_001080932.3): 5′-AATGCAGCAGCAA GTCCTCT-3′ and 5′-GCAATGACAATGCTCTCGCC-3′;

2.6. Northern blot

~20 μg total RNA was separated by 3% agarose gel and transferred onto a Blotting-Nylon 66 membrane (Sigma-Aldrich). Subsequent Northern blot was performed with a Digoxin-labelled locked nucleic acid probes (Exiqon, Shanghai, China) that had been prepared using the DIG Northern starter Kit (Roche, Shanghai, China), with the aid of NorthernMax kit (Ambion, Shanghai, China) following manufacturer instructions. Final visualization of positive signals was achieved through phosphorimaging (Typhoon, Mundelein, IL, USA).

2.7. RNA fluorescent in situ hybridization (RNA-FISH)

HUVECs were cultured to 80% confluence and then subjected to prehybridization (1 × PBS/0.5% Triton X-100). HUVECs were then incubated with FITC-labelled RNA probes to miR-140-3p in the hybridization buffer (ThermoFisherScientific, Shanghai, China) overnight. HUVECs were counter-stained using 4,6-diamidino-2-phenylindole (Sigma-Aldrich) and final positive signals were developed using RNAscope® Multiplex Assay Kit (ThermoFisherScientific).[25]

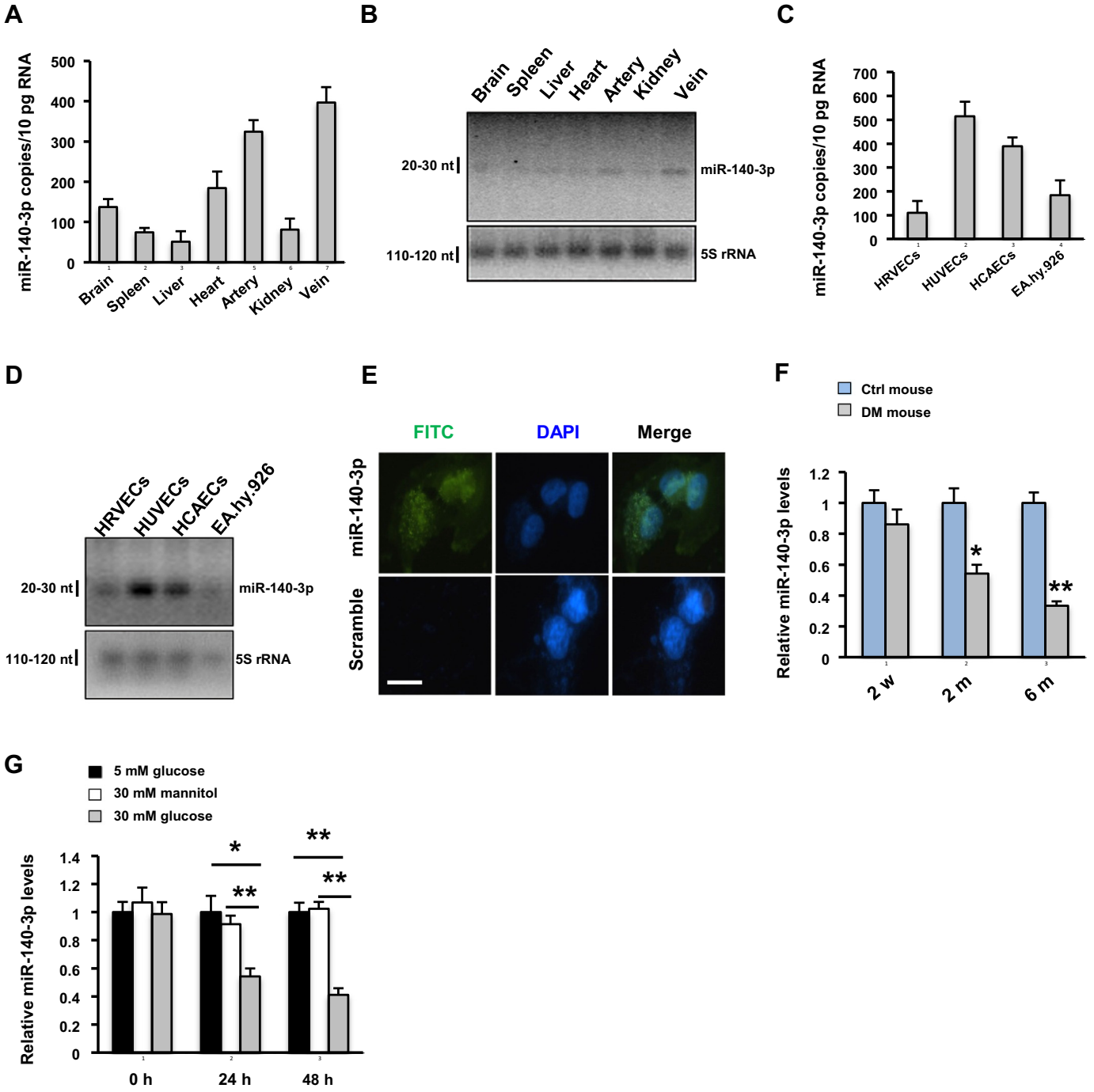

Fig. 1. High glucose challenges inhibits miR-140-3p expression in mouse tissues and ECs. (A) Total RNA was isolated from different mouse tissues using a miRNeasy Mini Kit as described in Materials and methods. Subsequently, absolute quantification of miR-140-3p expression in different mouse tissues was achieved using ($n = 4$). (B) Northern blot analysis of miR-140-3p expression in different mouse tissues ($n = 4$). (C) Absolute quantification of miR-140-3p expression in different endothelial cells ($n = 4$). (D) Northern blot analysis of miR-140-3p expression in different endothelial cells ($n = 4$). (E) Localization of miR-140-3p in HUVECs was revealed by RNA-FISH assay ($n = 3$). Bar = 10 μm (F) RT-qPCR analysis of miR-140-3p expression in the primary ECs isolated from normal and diabetic mice, at the end of different durations after DM induction ($n = 5$). $^{*}P < 0.05$ and $^{**}P < 0.01$ when compared to the Ctrl mouse. (G) HUVECs were incubated with the culture media containing 5 mmol/L glucose, 30 mmol/L glucose, or 30 mmol/L mannitol for the indicated durations, followed by RT-qPCR analysis ($n = 5$, $^{*}P < 0.05$ and $^{**}P < 0.01$).

2.8. Western blotting/immunoblotting

Immunoblotting was carried out according to our previous work.[12] Briefly, total protein samples were isolated from primary ECs or HUVECs using a ReadyPrep Protein Extraction Kit (Bio-Rad, Beijing, China) with the aid of the complete proteinase inhibitor cocktail tablets (Roche, Shanghai, China). A total of ~30 μg of protein samples were separated by SDS/PAGE and were transferred to a PVDF membrane (Bio-Rad), followed by incubation with the antibodies including rabbit-anti FOXK2 (1:1000, Sigma-Aldrich) and rabbit anti-β-ACTIN (Santa Cruz Biotechnology, Shanghai, China). Final signals were developed using an ECL kit (ThermoFisherScientific) according to the manufacturer's instructions.

2.9. Luciferase reporter assay

The FOXK2 3′UTR spanning 500 bp was PCR amplified from human genomic DNA using Taq DNA polymerase (Qiagen) and was

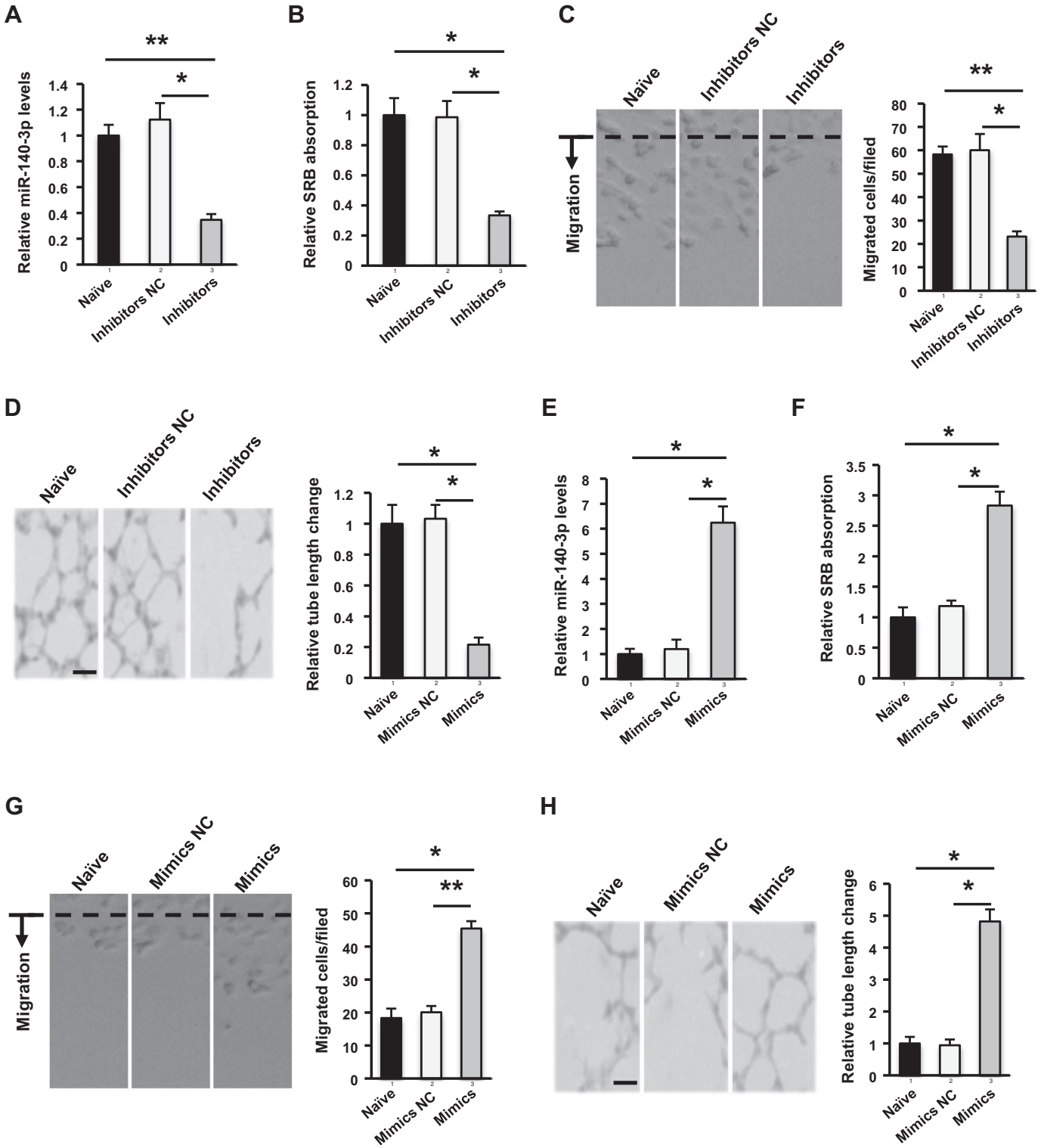

Fig. 2. miR-140-3p regulates the endothelial function *in vitro*. (A) Normal primary ECs were transfected with miR-140-3p inhibitors or negative controls (NC). 48 h later, normal primary ECs were subjected to RT-qPCR analysis of miR-140-3p expression ($n = 5$, $^{*}P < 0.05$ and $^{**}P < 0.01$). (B) Effects of miR-140-3p inhibition on the endothelial proliferation was determined using Sulforhodamine-B (SRB) absorption assay in normal primary ECs ($n = 5$). (C) Effects of miR-140-3p inhibition on the endothelial migration was evaluated using wound healing assay in normal primary ECs ($n = 5$). (D) Normal primary ECs with different transfections were seeded on the Matrigel matrix. 24 h later, tube construction was viewed and tube length was statistically analyzed ($n = 4$, $^{*}P < 0.05$ and $^{**}P < 0.01$). Scale bar = 50 μm (E) Diabetic primary ECs were transfected with miR-140-3p mimics or negative controls (NC). 48 h later, diabetic primary ECs were subjected to RT-qPCR analysis of miR-140-3p expression ($n = 5$, $^{*}P < 0.05$ and $^{**}P < 0.01$). (F) Effects of miR-140-3p overexpression on the endothelial proliferation was determined using SRB absorption assay in diabetic primary ECs ($n = 5$). (G) Effects of miR-140-3p overexpression on the endothelial migration was evaluated using wound healing assay in diabetic primary ECs ($n = 5$). (H) Effects of miR-140-3p overexpression on *in vitro* angiogenesis was evaluated using tube formation assay in diabetic primary ECs ($n = 4$, $^{*}P < 0.05$ and $^{**}P < 0.01$).

cloned into *Kpn*I–*Nhe*I sites of pGL4.10[luc2] Vector (Promega, Beijing, China) using CloneJET PCR Cloning Kit (Thermo Fisher Scientific). The site-directed mutagenesis was achieved using QuikChange II Site-Directed Mutagenesis Kit (Agilent, Beijing, China). The wild-type pGL4.10/FOXK2-3′UTR or mutated pGL4.10/FOXK2-3′UTR, along with empty vector, were cotransfected with pSV-β-galactosidase into NIH/3T3 cells. 24 h later, relative luciferase activity was measured using Dual-Glo Luciferase.

Reporter Assay kit (Promega).[26]

2.10. Statistical analysis

All data are presented as mean ± S.E.M. Statistical significance was assessed by performing *Student's t*-test or one way analysis of variance (ANOVA) as appropriate, using a *P*-value of 0.05. Correlation analysis between miR-140-3p expression and *FOXK2* transcripts level was achieved using the *Pearson Chi-Square* test.

3. Results

3.1. Down-regulation of miR-140-3p in high glucose conditions

Because has-miR-140-3p and mmu-miR-140-3p share the same sequence, we firstly explored the expression profile of miR-140-3p in different mouse tissues. RT-qPCR revealed that miR-140-3p was expressed in multiple tissues including brain, spleen, liver, heart, kidney, artery and vein, with the highest values being observed in artery and vein (Fig. 1A). This expression profile was further verified by Northern blotting using a LNA-labelled miR-140-3p probe (Fig. 1B). miR-140-3p expression was also abundantly detected in HUVECs and HCAECs, along with modest expression levels in other endothelial cells, as well, including HRVECs and EA.hy.926 (Fig. 1C and D). As expected, RNA-FISH showed that miR-140-3p was mainly expressed in the cytoplasm of HUVECs (Fig. 1E). Because we were interested in the potential role of miR-140-3p in the diabetic vascular complications, we then examined the miR-140-3p expression in the primary ECs from diabetic mice, which have been prepared and described in our previous work.[12] Our FACS analysis demonstrated that both PECAM-1 and ICAM-2, two endothelial-specific markers, were abundantly expressed in the primary ECs isolated from mouse hearts (Supplementary Fig. 1), thus validating the endothelial cell lineage in our system. RT-qPCR revealed that miR-140-3p expression in the primary ECs from diabetic mice was significantly lower than that from non-diabetic mice (Fig. 1F). Consistently, treatment with high-glucose in HUVECs could inhibit the expression levels of miR-140-3p in a time-dependent manner (Fig. 1G). Thus, hyperglycemia suppresses miR-140-3p expression at both *in vivo* and *in vitro* levels.

3.2. Endothelial miR-140-3p positively regulates angiogenesis

To address the biological significance of miR-140-3p as a regulator of angiogenesis, we transfected miR-140-3p inhibitors into normal primary ECs. 48 h later, the effectiveness of miR-140-3p knockdown was verified by RT-qPCR assay (Fig. 2A). Interestingly, miR-140-3p inhibition significantly impaired endothelial proliferation (average SRB absorption values 0.334 in ECs transfected with Inhibitors as compared to an overall average SRB absorption values of 0.986 in ECs transfected with Inhibitors NC, Fig. 2B) and migration (average migrated cell numbers 23.14 in the primary ECs transfected with Inhibitors as compared to an overall average migrated cell numbers 60.08 in the primary ECs transfected with Inhibitors NC, Fig. 2C), and thereby resulted in a compromised tube formation of primary ECs (Fig. 2D). By contrast, transfection of miR-140-3p mimics in diabetic primary ECs (Fig. 2E) abrogated high glucose-impaired endothelial proliferation (average SRB absorption values 2.834 in diabetic primary ECs transfected with Mimics as compared to an overall average SRB absorption values of 1.186 in diabetic primary ECs transfected with Mimics NC, Fig. 2F) and migration (average migrated cell numbers 45.44 in diabetic primary ECs transfected with Inhibitors as compared to an overall average migrated cell numbers 20.08 in diabetic primary ECs transfected with Inhibitors NC, Fig. 2G), thus rescuing the inhibitory effect of diabetes on *in vitro* angiogenesis in diabetic primary ECs (Fig. 2H).

3.3. miR-140-3p directly targets the 3′UTR of forkhead box K2 (FOXK2)

With the aid of TargetScan and miRDB, the 3′UTR of *FOXK2* gene was recognized as a putative target of miR-140-3p (Fig. 3A). A direct connection between miR-140-3p and FOXK2 was firstly substantiated when we assayed the relative transcript levels of FOXK2 in miR-140-3p mimics-transfected primary ECs. Diabetes resulted in a more than two-fold increase in the relative transcript levels of FOXK2 in primary ECs, whereas this stimulatory effect was substantially abolished upon transfection with miR-140-3p mimics, as evidenced by our immunoblotting (Fig. 3B) and RT-qPCR (Fig. 3C) analyses. Human circulating $CD34^+$ cells contain a large portion of endothelial progenitor cells.[12] *Pearson Chi-Square* test revealed a negative correlation between FOXK2 and miR-140-3p expression levels in the $CD34^+$ cells purified from the peripheral blood samples of DM patients (Fig. 3D). To provide the direct evidence for the regulation of FOXK2 expression by miR-140-3p, we cloned wild-type *FOXK2* 3′UTR and mutated *FOXK2* 3′UTR into luciferase reporter vector pGL4.10 (Fig. 3E). Transient cotransfection of miR-140-3p mimics and WT pGL4.10/FOXK2-3′UTR in NIH/3T3 cells resulted in a noticeable suppression of *FOXK2* transcript. Contrarily, suppression of *FOXK2* transcription by miR-140-3p mimics was completely abrogated when cells were transfected with Mu pGL4.10/FOXK2-3′UTR (Fig. 3F). To further ask whether FOXK2 alone can explain for the miR-140-3p deficiency-induced angiogenic dysfunction, we established HUVECs stably deprived of endogenous FOXK2 expression. As expected, transfection with miR-140-3p inhibitors failed to stimulate FOXK2 expression in HUVECs/shRNA (Fig. 3G). Importantly, FOXK2 inhibition efficiently rescued miR-140-3p deficiency-impaired endothelial proliferation (Fig. 3H) and tube formation capability (Fig. 3I) in HUVECs/shRNA. Taken together, these results indicate that miR-140-3p could regulate angiogenic function by directly targeting FOXK2 signaling.

3.4. Translation of miR-140-3p molecular effects to human disease

To further provide the translational medicine relevance for the effects of miR-140-3p on diabetic vascular disorders, we explored miR-140-3p levels in plasma and AH samples collected from diabetic patients and normal controls. miR-140-3p expression was significantly down-regulated in the plasma of peripheral blood from diabetic patients (Fig. 4A). Deregulation of AH, an important body fluid in the eye, is frequently associated with retinal

Fig. 3. miR-140-3p targets FOXK2. (A) Prediction of miR-140-3p binding site on the 3′UTR of *FOXK2*. 48 h after transfection, different primary ECs were subjected to Western blotting (B) and RT-qPCR analysis (C) to reveal the expression levels of FOXK2 ($n = 4$). (D) Correlation analysis between miR-140-3p and *FOXK2* mRNA in human $CD34^+$ cells ($n = 4$). (E) Schematic diagram of *FOXK2* 3′-UTR reporter construct. (F) Luciferase reporter assay showing that miR-140-3p directly repressed *FOXK2* transactivation ($n = 4$). (G) HUVECs were stably deprived of endogenous FOXK2 expression by transfection with FOXK2 shRNA. Cells were then transfected with miR-140-3p inhibitors or NC for 48 h, followed by immunoblotting analysis ($n = 4$). (H) HUVECs with different transfections were subjected to SRB absorption assay to determine the effects of FOXK2 inhibition, in the presence or absence of miR-140-3p inhibition, on endothelial proliferation ($n = 5$, $^*P < 0.05$ and $^{**}P < 0.01$). (I) Effects of FOXK2 inhibition, in the presence or absence of miR-140-3p inhibition, on *in vitro* angiogenesis was evaluated using tube formation assay in HUVECs with different transfections ($n = 4$, $^*P < 0.05$ and $^{**}P < 0.01$).

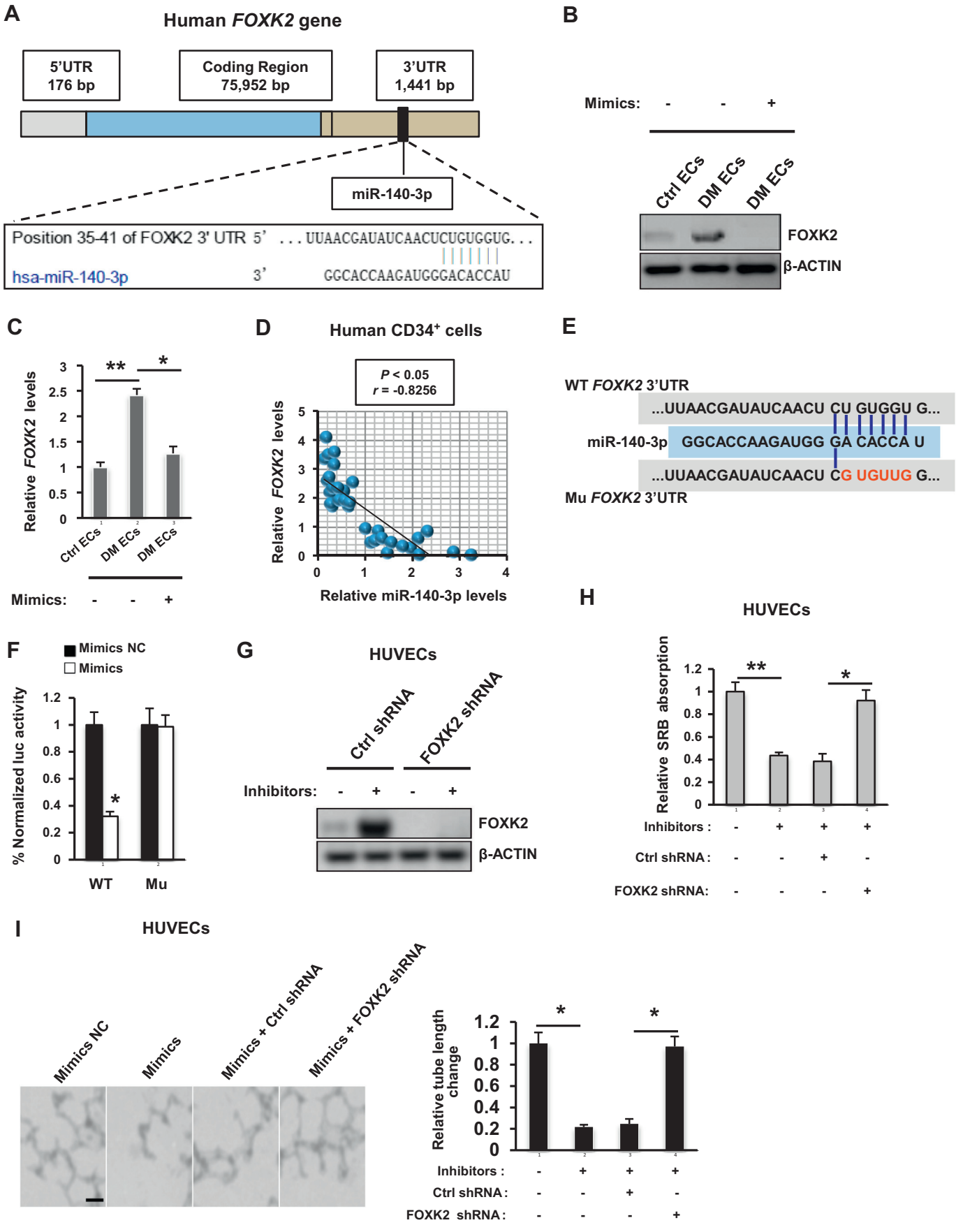
A
Human FOXK2 gene
5'UTR
176 bp
Coding Region
75,952 bp
3'UTR
1,441 bp
miR-140-3p
Position 35-41 of FOXK2 3' UTR 5' ...UUAACGAUAUCAACUCUGUGGUG...
hsa-miR-140-3p 3' GGCACCAAGAUGGGACACCAU
B
Mimics: - - +
Ctrl ECs
DM ECs
DM ECs
FOXK2
β-ACTIN
C
Relative FOXK2 levels
Ctrl ECs
DM ECs
DM ECs
Mimics: - - +
D
Human CD34+ cells
P < 0.05
r = -0.8256
Relative FOXK2 levels
Relative miR-140-3p levels
E
WT FOXK2 3'UTR
...UUAACGAUAUCAACU CU GUGGU G...
miR-140-3p GGCACCAAGAUGG GA CACCA U
...UUAACGAUAUCAACU CG UGUUG G...
Mu FOXK2 3'UTR
F
Mimics NC
Mimics
% Normalized luc activity
WT
Mu
G
HUVECs
Ctrl shRNA
FOXK2 shRNA
Inhibitors: - + - +
FOXK2
β-ACTIN
H
HUVECs
Relative SRB absorption
Inhibitors : - + + +
Ctrl shRNA : - - + -
FOXK2 shRNA: - - - +
I
HUVECs
Mimics NC
Mimics
Mimics + Ctrl shRNA
Mimics + FOXK2 shRNA
Relative tube length change
Inhibitors : - + + +
Ctrl shRNA : - - + -
FOXK2 shRNA : - - - +

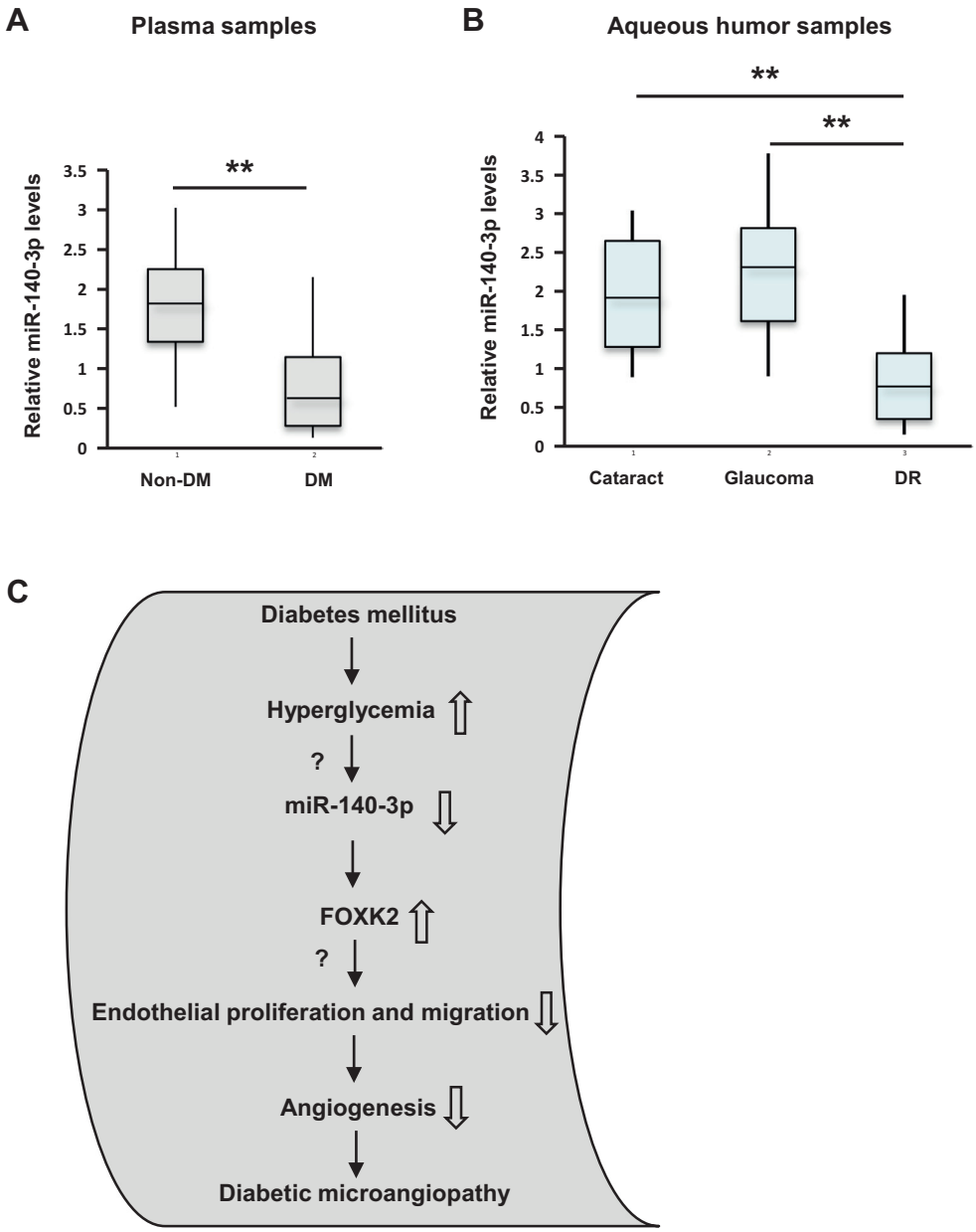

Fig. 4. Translation of miR-140-3p molecular effects to human disease. (A) Relative miR-140-3p expression in the plasma of peripheral blood from diabetic patients and nondiabetic controls was determined using RT-qPCR analysis ($n = 4$, $^{*}P < 0.05$ and $^{**}P < 0.01$). (B) RT-qPCR analysis of miR-140-3p expression levels in aqueous humor (AH) of patients with cataract, glaucoma, and diabetic retinopathy (DR) ($n = 4$, $^{*}P < 0.05$ and $^{**}P < 0.01$). (C) Proposed working model for the putative effects of high glucose inhibition on miR-140-3p-mediated FOXK2 signaling leading to diabetic microvascular complications.

microvascular diseases.[22] Interestingly, miR-140-3p expression was significantly reduced in the AH of patients with diabetic retinopathy, but not in other patients with cataract or glaucoma (Fig. 4B). Thus, circulating miR-140-3p may serve as a potent biofluid derived-biomarker for monitoring microvascular complications in diabetic patients.

4. Discussion

Although accumulating evidence suggests that deregulation of miRNAs is a hallmark of vascular disorders caused by diabetes, only minor studies have characterized the biological effects and corresponding mechanisms of distinct miRNAs. The data presented here show that miR-140-3p expression is significantly attenuated in primary ECs upon hyperglycemia stimulation. miR-140-3p inhibition compromises the angiogenic function in primary ECs by directly targeting FOXK2 signaling. Conversely, repression of FOXK2 rescues the miR-140-3p deficiency-impaired angiogenesis in HUVECs. miR-140-3p/FOXK2 cascade thus mediates, at least in part, the angiogenic dysfunction in diabetes.

Based on our data, miR-140-3p has a "positive" effect on angiogenesis, and its inhibition by DM conditions leads to decreased angiogenesis. However, diabetic retinopathy, a secondary microvascular complication of DM, is characterized by two hallmarks: diabetic macular edema and increased retinal blood vessel growth and angiogenesis.[27] Therefore, could inhibition of miR-140-3p instead be positive for diabetic retinopathy? Three possibilities may account for this intriguing question: 1) In our study, we constantly observed that the expression levels of miR-140-3p were almost negligible in HRVECs, as compared to those in other cell types (Fig. 1C and D). We thus could not rule out the

possibility that miR-140-3p may not be responsible for the angiogenic regulation in retinopathy. It is well recognized that the functions of many miRNAs are determined by the cell context and tissue types.[28] 2) Although the angiogenesis or neovascularization is elevated in diabetic retinopathy, most of the newly-formed vessels inside the retina demonstrate abnormal architecture and permeability.[29] Therefore, it is likely that miR-140-3p may not function as an essential regulator of vessel formation. Instead, dysregulation of miR-140-3p signaling may directly target the vascular structure and function. 3) It is well known that DM exerts differential effects on angiogenic process in different tissue types. For example, in four limbs, DM attenuates angiogenic response to tissue injury, thus contributing crucially to the strong propensity to develop persistent decubitus and foot ulcers.[21] By contrast, the growth of new blood vessels in retina is significantly enhanced by DM, which, if not properly controlled, leads to irreversible retinal damages and vision loss.[30,31] Thus, the proangiogenic and antiangiogenic effects by DM can both promote vascular dysfunction in different tissue types. Therefore, miR-140-3p may also serve as a double-faced regulator angiogenic function in different tissues. These interesting hypotheses are currently under investigation in our lab.

miR-140-3p has recently gained much attention due to its regulatory roles in metabolic processes.[17] To this end, we show here that hyperglycemia is associated with decreased expression levels of miR-140-3p in both cultured primary ECs and diabetic human blood samples. Our results are well consistent with the previous studies in which miR-140-3p are demonstrated to be significantly down-regulated in impaired fracture healing[16] and progressive chronic kidney disease in diabetes.[32] It is therefore clear that hyperglycemia modifies the changes to the miR-140-3p expression pattern, but mechanistically the details remain to be further resolved. A role for intracellular oxidative stress in mediating hyperglycemia inhibition on endothelial miR-140-3p is very likely, given the prooxidative environment in diabetic ECs. Diabetes impairs glucose uptake and metabolic substrate shifts, thus leading to a substantial oxidative stress. The latter has been well documented to be a potent agent of post-translational modification in diabetes microvascular pathology.[33] Excessive reactive oxygen species (ROS) can cause regulatory effects through oxidative modification of miRNA leading to their deregulated expressions and functions. For example, maternal diabetes induces miR-27a expression, which causes ROS imbalance by directly targeting Nrf2 singling in diabetic embryopathy.[34] Likewise, Angiotensin II, a well-known pro-oxidant induced by hyperglycaemia, suppresses miR-145 expression and thereby promotes cardiomyocyte apoptosis and aggravates infarcted myocardium.[35] Thus, we propose a model of coordinate regulation by hyperglycemia and oxidative stress-induced repression of miR-140-3p in ECs. This tempting possibility is currently under investigation in our lab.

Intriguingly, our functional analyses reveal that inhibition of endogenous miR-140-3p impairs EC proliferation, migration, and angiogenic potentials in primary ECs. By contrast, forced miR-140-3p expression restored endothelial proliferation and potentiates *in vitro* angiogenesis in diabetic primary ECs. miR-140-3p may thus act as an essential promoter of neovascularization in primary ECs. In favor of this hypothesis, it has been shown that miR-140-5p inhibits angiogenesis by decreasing endothelial proliferation, migration and tube formation, in both cerebral ischemia[14] and breast cancers.[15] Thus, regulation of angiogenesis appears to be a fundamental function of miR-140 family, but different members may exert differential regulatory roles under different pathophysiological conditions.

Revealing the direct down-stream targets is essential before interfering with miRNA expression for therapeutic purposes.[5] By employing multiple approaches including bioinformatics analysis, luciferase reporter assay and site-directed mutagenesis, we have identified FOXK2 as a potential target of miR-140-3p in primary ECs and HUVECs. Emerging data suggest that the forkhead transcription factors regulate fundamentally the angiogenic function. For instance, endothelial FOXO1 is an intrinsic regulator restraining angiogenesis in ischemic muscle.[36] FOXP3 inhibits angiogenesis by downregulating VEGF in breast cancer.[37] Together, the forkhead transcription factors are conserved angiogenic regulators in both normal and transformed cells.[38] Of particular interest, the regulation of forkhead transcription factors is tightly controlled at posttranscriptional levels by miRNAs. miR-544a and miR-379 regulates the angiogenesis in ECs by directly targeting FOXP1 and FOXP2 pathways, respectively.[39] miR-370 potentiates neovascularization in amputated fingers through targeting FOXO1 signaling.[40] As for FOXK2, it is targeted by miR-1271-5p and may promote cell growth and unfavorable prognosis in hepatocellular carcinoma.[41] The current study extends these understandings by identifying FOXK2 as the direct target of miR-140-3p in primary ECs and HUVECs. To the best of our knowledge, this is the first demonstration of a specific miRNA regulation of FOXK2 in diabetic vascular implications.

In summary, we show here that miR-140-3p has an inhibitory effect on FOXK2 expression, which potentiates angiogenic function and promote *in vitro* tube formation in endothelial cells. Deregulation of miR-140-3p/FOXK2 cascade is therefore implicated in the pathogenesis of diabetes-associated vascular complications (Fig. 4C). miRNAs are protected from RNase, and are usually stable in bio-fluid samples.[5] In line with this insight, the expression levels of miR-140-3p in plasma and AH were significantly decreased in diabetic patients, rendering the possibility of using miR-140-3p as a suitable bio-fluid derived-biomarker for evaluating different diabetic conditions.

Supplementary data to this article can be found online at https://doi.org/10.1016/j.jdiacomp.2019.02.001.

Declarations of interest

None.

Acknowledgments

We appreciate the constant technical support from Department of Ophthalmology in 3rd People's Hospital of Qingdao.

Author contributions

Conceived and designed the experiments: S-Y. C.
Performed the experiments: D-N. W., H-Y. W., C.L., X-F.M., S-Y.C.
Analyzed the data: D-N. W., H-Y. W., C.L., X-F.M., S-Y.C.
Contributed reagents/materials/analysis tools: D-N. W., H-Y. W., S-Y.C.
Wrote the paper: S-Y. C.

Funding

This study received no funding support.

Conflicts of interest

There are no relevant conflicts of interest to disclose.

References

1. Lee KW, Ching SM, Ramachandran V, et al. Prevalence and risk factors of gestational diabetes mellitus in Asia: a systematic review and meta-analysis. BMC Pregnancy Childbirth 2018;18:494.
2. Gutierrez J, Alloubani A, Mari M, Alzaatreh M. Cardiovascular disease risk factors: hypertension, diabetes mellitus and obesity among Tabuk citizens in Saudi Arabia. Open Cardiovasc Med J 2018;12:41-9.
3. Domingueti CP, Dusse LM, Carvalho M, de Sousa LP, Gomes KB, Fernandes AP. Diabetes mellitus: the linkage between oxidative stress, inflammation, hypercoagulability and vascular complications. J Diabetes Complications 2016;30:738-45.
4. Bakker EJ, Valentijn TM, van de Luijtgaarden KM, et al. Type 2 diabetes mellitus, independent of insulin use, is associated with an increased risk of cardiac complications after vascular surgery. Anaesth Intensive Care 2013;41:584-90.
5. Caporali A, Meloni M, Vollenkle C, et al. Deregulation of microRNA-503 contributes to diabetes mellitus-induced impairment of endothelial function and reparative angiogenesis after limb ischemia. Circulation 2011;123:282-91.

6. Xu P, Guan MP, Bi JG, Wang D, Zheng ZJ, Xue YM. High glucose down-regulates microRNA-181a-5p to increase pro-fibrotic gene expression by targeting early growth response factor 1 in HK-2 cells. Cell Signal 2017;31:96-104.
7. Zhang HN, Xu QQ, Thakur A, et al. Endothelial dysfunction in diabetes and hypertension: role of microRNAs and long non-coding RNAs. Life Sci 2018;213:258-68.
8. Sliwinska A, Kasinska MA, Drzewoski J. MicroRNAs and metabolic disorders - where are we heading? Arch Med Sci 2017;13:885-96.
9. Banerjee J, Nema V, Dhas Y, Mishra N. Role of MicroRNAs in type 2 diabetes and associated vascular complications. Biochimie 2017;139:9-19.
10. Li H, Liu J, Wang Y, et al. MiR-27b augments bone marrow progenitor cell survival via suppressing the mitochondrial apoptotic pathway in type 2 diabetes. Am J Physiol Endocrinol Metab 2017;313:E391-401.
11. Rawal S, Munasinghe PE, Shindikar A, et al. Down-regulation of proangiogenic microRNA-126 and microRNA-132 are early modulators of diabetic cardiac microangiopathy. Cardiovasc Res 2017;113:90-101.
12. Cheng S, Cui Y, Fan L, Mu X, Hua Y. T2DM inhibition of endothelial miR-342-3p facilitates angiogenic dysfunction via repression of FGF11 signaling. Biochem Biophys Res Commun 2018;503:71-8.
13. Long J, Wang Y, Wang W, Chang BH, Danesh FR. Identification of microRNA-93 as a novel regulator of vascular endothelial growth factor in hyperglycemic conditions. J Biol Chem 2010;285:23457-65.
14. Sun J, Tao S, Liu L, Guo D, Xia Z, Huang M. miR1405p regulates angiogenesis following ischemic stroke by targeting VEGFA. Mol Med Rep 2016;13:4499-505.
15. Lu Y, Qin T, Li J, et al. MicroRNA-140-5p inhibits invasion and angiogenesis through targeting VEGF-A in breast cancer. Cancer Gene Ther 2017;24:386-92.
16. Takahara S, Lee SY, Iwakura T, et al. Altered expression of microRNA during fracture healing in diabetic rats. Bone Joint Res 2018;7:139-47.
17. Ntoumou E, Tzetis M, Braoudaki M, et al. Serum microRNA array analysis identifies miR-140-3p, miR-33b-3p and miR-671-3p as potential osteoarthritis biomarkers involved in metabolic processes. Clin Epigenetics 2017;9:127.
18. Tanaka Y, Tsuda S, Kunikata H, et al. Profiles of extracellular miRNAs in the aqueous humor of glaucoma patients assessed with a microarray system. Sci Rep 2014;4:5089.
19. Kim TH, Kim MK, Cheong YH, et al. Hepatic role in an early glucose-lowering effect by a novel dipeptidyl peptidase 4 inhibitor, evogliptin, in a rodent model of type 2 diabetes. Eur J Pharmacol 2016;771:65-76.
20. Lim YC, Garcia-Cardena G, Allport JR, et al. Heterogeneity of endothelial cells from different organ sites in T-cell subset recruitment. Am J Pathol 2003;162:1591-601.
21. Sawada N, Jiang A, Takizawa F, et al. Endothelial PGC-1alpha mediates vascular dysfunction in diabetes. Cell Metab 2014;19:246-58.
22. Shan K, Liu C, Liu BH, et al. Circular noncoding RNA HIPK3 mediates retinal vascular dysfunction in diabetes mellitus. Circulation 2017;136:1629-42.
23. Yang J, Kim WJ, Jun HO, et al. Hypoxia-induced fibroblast growth factor 11 stimulates capillary-like endothelial tube formation. Oncol Rep 2015;34:2745-51.
24. Dong YS, Hou WG, Li Y, et al. Unexpected requirement for a binding partner of the syntaxin family in phagocytosis by murine testicular Sertoli cells. Cell Death Differ 2016;23:787-800.
25. Bai YP, Zhang JX, Sun Q, Zhou JP, Luo JM, He LF, Lin XC, Zhu LP, Wu WZ, Wang ZY, Zhang GG. nduction of microRNA-199 by Nitric Oxide in Endothelial Cells Is Required for Nitrovasodilator Resistance via Targeting of Prostaglandin I2 Synthase. Circulation 2018;138(4):397-411, https://doi.org/10.1161/CIRCULATIONAHA.117.029206.
26. Yu L, Su YS, Zhao J, Wang H, Li W. Repression of NR4A1 by a chromatin modifier promotes docetaxel resistance in PC-3 human prostate cancer cells. FEBS Lett 2013;587:2542-51.
27. Crawford TN, Alfaro 3rd DV, Kerrison JB, Jablon EP. Diabetic retinopathy and angiogenesis. Curr Diabetes Rev 2009;5:8-13.
28. Zhao G, Li Y, Wang T. Potentiation of docetaxel sensitivity by miR-638 via regulation of STARD10 pathway in human breast cancer cells. Biochem Biophys Res Commun 2017;487:255-61.
29. Tremolada G, Del Turco C, Lattanzio R, et al. The role of angiogenesis in the development of proliferative diabetic retinopathy: impact of intravitreal anti-VEGF treatment. Exp Diabetes Res 2012;2012, 728325.
30. Lau JC, Kroes RA, Moskal JR, Linsenmeier RA. Diabetes changes expression of genes related to glutamate neurotransmission and transport in the Long-Evans rat retina. Mol Vis 2013;19:1538-53.
31. Lasta M, Pemp B, Schmidl D, et al. Neurovascular dysfunction precedes neural dysfunction in the retina of patients with type 1 diabetes. Invest Ophthalmol Vis Sci 2013;54:842-7.
32. Rudnicki M, Perco P. B DH, et al. renal microRNA- and RNA-profiles in progressive chronic kidney disease. Eur J Clin Invest 2016;46:213-26.
33. Wang JX, Gao J, Ding SL, et al. Oxidative modification of miR-184 enables it to target Bcl-xL and Bcl-w. Mol Cell 2015;59:50-61.
34. Zhao Y, Dong D, Reece EA, Wang AR, Yang P. Oxidative stress-induced miR-27a targets the redox gene nuclear factor erythroid 2-related factor 2 in diabetic embryopathy. Am J Obstet Gynecol 2018;218(1): 136 e131–136 e110.
35. Wang BW, Fang WJ, Shyu KG. MicroRNA-145 regulates disabled-2 and Wnt3a expression in cardiomyocytes under hyperglycaemia. Eur J Clin Invest 2018;48.
36. Ren B, Best B, Ramakrishnan DP, Walcott BP, Storz P, Silverstein RL. LPA/PKD-1-FoxO1 signaling axis mediates endothelial cell CD36 transcriptional repression and proangiogenic and proarteriogenic reprogramming. Arterioscler Thromb Vasc Biol 2016;36:1197-208.
37. Li X, Gao Y, Li J, et al. FOXP3 inhibits angiogenesis by downregulating VEGF in breast cancer. Cell Death Dis 2018;9:744.
38. Maiese K, Hou J, Chong ZZ, Shang YC. A fork in the path: developing therapeutic inroads with FoxO proteins. Oxid Med Cell Longev 2009;2:119-29.
39. He Q, Zhao L, Liu Y, et al. Circ-SHKBP1 regulates the angiogenesis of U87 glioma-exposed endothelial cells through miR-544a/FOXP1 and miR-379/FOXP2 pathways. Mol Ther Nucleic Acids 2018;10:331-48.
40. Zhang H, Sun X, Hao D. Upregulation of microRNA-370 facilitates the repair of amputated fingers through targeting forkhead box protein O1. Exp Biol Med (Maywood) 2016;241:282-9.
41. Lin MF, Yang YF, Peng ZP, et al. FOXK2, regulated by miR-1271-5p, promotes cell growth and indicates unfavorable prognosis in hepatocellular carcinoma. Int J Biochem Cell Biol 2017;88:155-61.